# Quantum gate using qubit states separated by terahertz

Kenji Toyoda,[1,2] Shinsuke Haze,[1] Rekishu Yamazaki,[2] and Shinji Urabe[1,2]
[1]*Graduate School of Engineering Science, Osaka University, 1-3 Machikaneyama, Toyonaka, Osaka 560-8531, Japan*
[2]*JST-CREST, 4-1-8 Honmachi, Kawaguchi, Saitama 331-0012, Japan*
(Received 28 November 2009; published 24 March 2010)

A two-qubit quantum gate is realized using electronically excited states in a single ion with an energy separation on the order of a terahertz times the Planck constant as a qubit. Two phase-locked lasers are used to excite a stimulated Raman transition between two metastable states $D_{3/2}$ and $D_{5/2}$ separated by 1.82 THz in a single trapped $^{40}Ca^{+}$ ion to construct a qubit, which is used as the target bit for the Cirac-Zoller two-qubit controlled NOT gate. Quantum dynamics conditioned on a motional qubit is clearly observed as a fringe reversal in Ramsey interferometry.

DOI: 10.1103/PhysRevA.81.032322 PACS number(s): 03.67.Lx, 32.80.Qk, 37.10.Ty, 42.50.Ex

## I. INTRODUCTION

Atomic systems including trapped ions and neutral atoms are considered attractive for quantum information processing (QIP) since they can be made to be well isolated from the environment and hence enable construction of qubits with small decoherence or dephasing. Among experimental approaches toward QIP using different physical systems, some of the most advanced have been experiments using trapped ions [1,2], which are based on qubit levels with separation in the rf or microwave region or in the optical region. Recent advances in optical comb generation and optical frequency metrology [3–5] offer much flexibility in choosing qubit states, including atomic states with frequency separations that have not been explored before.

In view of recent progress in experiments on ultracold molecules transferred to the ground state of both internal and external degrees of freedom, molecular systems, which have rich internal structures, are also considered attractive for application to QIP. In the recent works [6–9], by performing stimulated Raman adiabatic passage using two lasers with high relative coherence, weakly bound ultracold Feshbach molecules are transferred to their rovibronic ground state. In addition, there are proposals to encode qubits in molecular states with small dipole moments and transfer these to states with larger dipole moments, thereby realizing switchable interaction between molecular qubits [10–13]. The required transfer can be performed by applying two phase-locked lasers through a stimulated Raman process.

In this article, we present the result of a quantum gate experiment using phase-locked lasers to excite a stimulated Raman transition. Two metastable states $D_{3/2}$ and $D_{5/2}$ in $^{40}Ca^{+}$ separated by 1.82 THz, each of which has a lifetime of $\sim$1.2 s [14], are used as the target bit to perform the Cirac-Zoller gate [15]. This is an attempt to use phase-locked lasers to bridge an energy separation larger than a terahertz and realize a quantum gate, and it is an important step toward obtaining a wider choice of qubit levels including internal levels of atoms and molecules.

Cirac and Zoller proposed in 1995 a realistic scheme for scalable quantum computation using a string of ions in a linear trap [15]. It was experimentally demonstrated in a simplified form using internal states and a motional degree of freedom in a single $^{9}Be^{+}$ ion [16]. A full implementation of the scheme in a scalable manner using a $^{40}Ca^{+}$ ion string with the technique of individual addressing was reported in 2003 [17].

It has been shown that all unitary operations on arbitrary many qubits can be decomposed into two-bit gates and one-bit gates [18]. One example of such a decomposition of unitary operations uses controlled NOT (CNOT) gates and rotation operations on single qubits [19,20]. Analogously to a classical exclusive-OR (XOR) gate, a CNOT quantum gate realizes the following operation: $|\epsilon_1\rangle|\epsilon_2\rangle \rightarrow |\epsilon_1\rangle|\epsilon_1 \oplus \epsilon_2\rangle$ with $\epsilon_{1,2} = 0, 1$ and $\oplus$ representing an addition modulo 2.

In the Cirac-Zoller (CZ) proposal [15], for implementing this CNOT operation, a red-sideband pulse, which is detuned to the lower side of the resonance of the qubit transition by the frequency of a collective motional mode, is applied between one basis state of the target qubit and an auxiliary state. When the collective motional state has one quantum, the red-sideband pulse applied for a duration corresponding to a $2\pi$ rotation causes a $\pi$ phase shift between two basis states of the target qubit states. On the other hand, when the collective motional state has no quantum, such rotation does not occur and no phase shift is given to the target qubit. This corresponds to a unitary operation conditioned on the motional quantum number, thereby implementing a controlled phase gate, and a CNOT gate is realized when this is combined with certain single-qubit operations.

## II. EXPERIMENTAL PROCEDURE

To realize the CZ gate using the metastable states in $^{40}Ca^{+}$ and its motional states, we adopt an excitation scheme using the stimulated Raman transition between $D_{3/2}$ and $D_{5/2}$ along with a quadrupole transition that connects the ground state $S_{1/2}$ with $D_{5/2}$ (see Fig. 1). The stimulated Raman transition is used for single-qubit operation on the metastable states, while the quadrupole transition is used for realizing the conditional phase shift required for a CZ gate, as well as sideband cooling and state preparation. As the target qubit states $|\uparrow\rangle \equiv D_{5/2}(m_J = 1/2)$ and $|\downarrow\rangle \equiv D_{3/2}(m_J = 1/2)$ are chosen, while as the control qubit the two low-lying states of the axial motion initialized to the ground state are used: $|0\rangle(|1\rangle) \equiv |n_z = 0\rangle(|n_z = 1\rangle)$, where $n_z$ denotes the axial motional quantum number. A conditional phase shift is implemented by applying a blue-sideband (BSB) $2\pi$ pulse

 

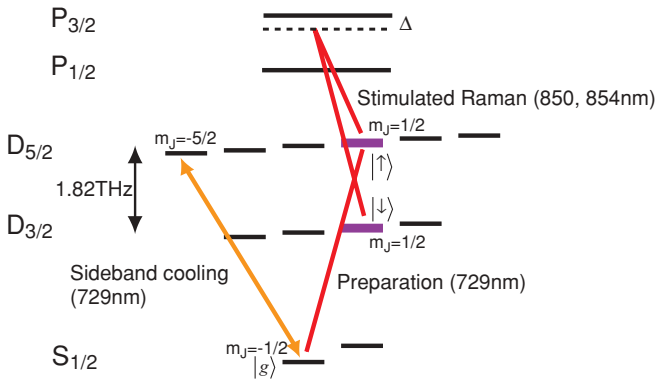


FIG. 1. (Color online) Level scheme for $^{40}Ca^{+}$ and transitions relevant for implementing the CZ gate. Two sublevels each from $D_{3/2}$ and $D_{5/2}$ metastable states, $|\uparrow\rangle \equiv |D_{5/2}(m_J = 1/2)\rangle$ and $|\downarrow\rangle \equiv |D_{3/2}(m_J = 1/2)\rangle$, are used as the qubit states here.

between $|\uparrow\rangle$ and $|g\rangle \equiv S_{1/2}(m_J = -1/2)$ state, which gives a $\pi$ phase shift to the $|1\rangle|\uparrow\rangle$.

We use a single $^{40}Ca^{+}$ ion trapped in a vacuum pressure of $6 \times 10^{-9}$ Pa. The trap used here is a conventional linear trap with an operating frequency of 23 MHz and secular frequencies of $(\omega_x, \omega_y, \omega_z)/2\pi = (1.91, 1.68, 0.72)$ MHz. A magnetic field of $\sim 3.1 \times 10^{-4}$ T is applied to lift the degeneracy of Zeeman states and to define the quantization axis for optical pumping. To reduce the effects of the ambient ac magnetic field, the vacuum chamber is enclosed in a magnetic shield. Loading of single ions is performed by using two-step photoionization from the $4s4s\ ^1S_0$ ground state of Ca via $4s4p\ ^1P_1$ with corresponding wavelengths of 423 and 375 nm for the first and second steps of the photoionization, respectively.

The setup of the phase-locked lasers used for excitation of the stimulated Raman transition has been modified from the one described in our previous article [21] in order to improve the noise in the difference frequency of the two lasers. Two Ti:sapphire lasers at 850 and 854 nm, phase-locked by using a passive-type optical comb [5] in combination with an acousto-optic modulator (AOM) and an electro-optic modulator [22], are used to excite the stimulated Raman transition. For excitation of the quadrupole transition, we use a titanium sapphire laser at 729 nm, which is stabilized to a high-finesse low-thermal-expansion cavity and has a linewidth of $<$400 Hz and a root-mean-square intensity noise of 0.3%. Control of optical frequency, phase, and amplitude is done by AOMs and the rf fields used for them are generated by direct-digital synthesis (DDS) boards, which are controlled by a field-programmable gate array (FPGA).

See Fig. 2 for the details of the beam configuration. For realizing gate experiments, all the motional degrees of freedom are cooled to near the ground states using Doppler cooling (with 397- and 866-nm lasers) and sideband cooling (SBC). For SBC, the $S_{1/2}(m_J = -1/2)$–$D_{5/2}(m_{J'} = -5/2)$ transition at 729 nm is used, and an additional quenching laser resonant to $D_{5/2}$–$P_{3/2}$ at 854 nm is also applied. All three dimensions are cooled for 2 ms each and this is repeated 20 times. Optical pumping is performed using the 397-nm $\sigma^-$ transition in

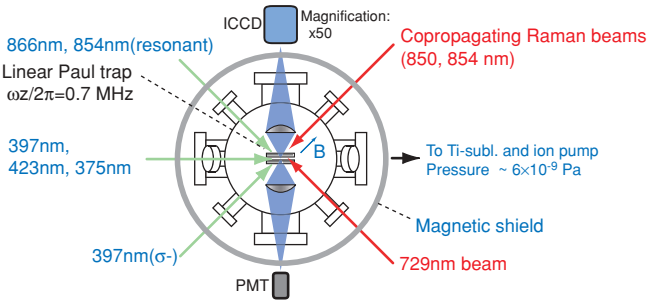


FIG. 2. (Color online) Experimental setup for the terahertz qubit quantum-gate experiment. See text for details.

$S_{1/2}(m_J = +1/2)$–$P_{1/2}(m_{J'} = -1/2)$ every 6 ms during SBC with a duration of 6 $\mu$s. The final quantum numbers obtained after SBC are $(\overline{n_x}, \overline{n_y}, \overline{n_z}) \sim (1, 1, 0.02)$.

For preparation to the $|\uparrow\rangle|0\rangle$ ($|\uparrow\rangle|1\rangle$) state, a carrier (BSB) $\pi$ pulse on $|g\rangle$–$|\uparrow\rangle$ is applied. This is a $|\Delta m_J| = 1$ transition, which requires a polarization different from that used for sideband cooling transition for which $|\Delta m_J| = 2$. In our case the former is parallel with and the latter is perpendicular to the surface of the optical table on which the trap chamber is placed (see Fig. 2). In order to perform both in one configuration, the polarization of the 729-nm light is chosen to be linear and rotated from the perpendicular direction by 45 degrees.

The target qubit states are discriminated by shining the cooling lasers at 397 and 866 nm for 7 ms and observing fluorescence photons by a photomultiplier.

The coherence times of the Raman transition have been measured to be $\sim$5.1 ms (1.6 ms) with (without) spin echo in a setup without a magnetic shield [23]. The coherence time for the quadrupole transition with a magnetic shield, which is deduced from decay of Rabi oscillation signals, is about 0.8 ms.

## III. RESULTS

### A. Rabi oscillation on the relevant transitions

Figure 3 shows Rabi oscillation signals on the relevant transitions including the carrier or BSB on $|g\rangle$–$|\uparrow\rangle$ and the carrier on the stimulated Raman transition. Based on these results, we can expect nearly unit fidelity for carrier pulses on $|g\rangle$–$|\uparrow\rangle$ while less fidelity for BSB Rabi pulses and carrier pulses on the stimulated Raman transition. The figure also shows results of numerical simulation, the details of which are given later. By comparing the simulation with the experiment, we can quantitatively characterize the fidelity-limiting factors, and this helps provide an estimation of the possible fidelity of Bell state generation as described later.

### B. Results for the Cirac-Zoller gate experiment

Figure 4(a) shows the pulse sequence for the Cirac-Zoller gate experiment. The first pulse (*preparation pulse*) is applied either on the carrier or BSB on $|g\rangle$–$|\uparrow\rangle$ to prepare the motional state $|0\rangle$ or $|1\rangle$, respectively. Then the first stimulated-Raman $\pi/2$ pulse is applied, which is followed by a BSB $2\pi$ pulse on $|g\rangle$–$|\uparrow\rangle$ and the second stimulated-Raman $\pi/2$ pulse. For $|0\rangle$ preparation the BSB $2\pi$ pulse causes no effect since there is

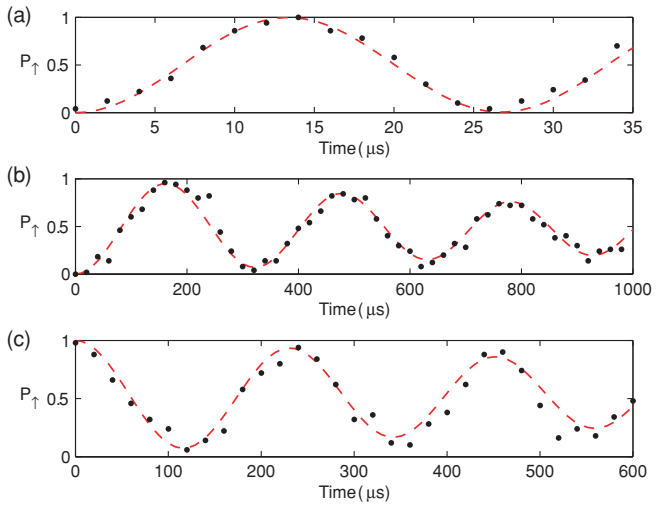


FIG. 3. (Color online) Rabi oscillation signals in the transitions relevant to the terahertz qubit scheme. (a) Carrier (BSB) Rabi oscillation and (b) BSB Rabi oscillation in $|g\rangle$–$|\uparrow\rangle$. (c) Carrier Rabi oscillation in the stimulated Raman transition $|\uparrow\rangle$–$|\downarrow\rangle$. The dashed curves are results of numerical simulation.

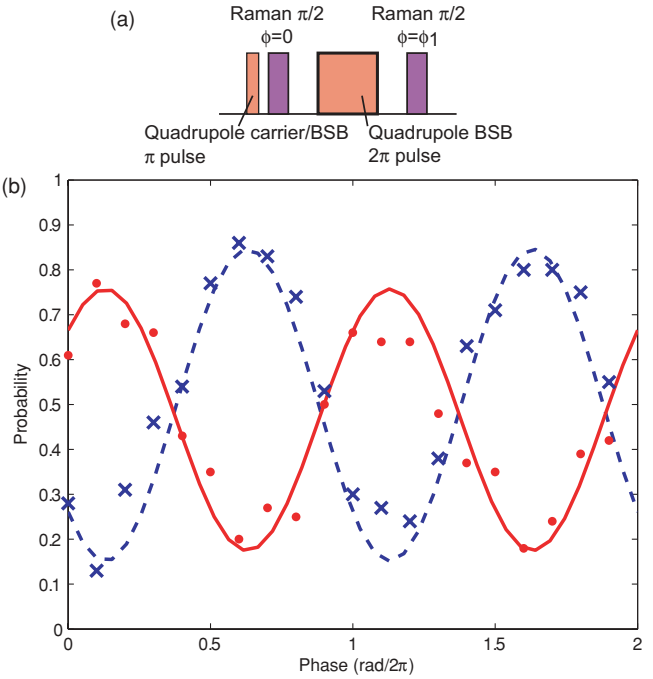


FIG. 4. (Color online) (a) Pulse sequence for the Cirac-Zoller gate experiment. (b) Result of a Cirac-Zoller gate experiment. Ramsey interference signals are plotted against the phase of the second pulse. Crosses (filled circles) represent the $|0\rangle$ ($|1\rangle$) preparation case. The solid (dashed) curve represents numerical simulation for $|0\rangle$ ($|1\rangle$) preparation. The $\pi$ phase difference between interference fringes indicates that a controlled dynamics characterizing the Cirac-Zoller gate is realized.

no motional state to reach in $|g\rangle$, while for $|1\rangle$ preparation the BSB $2\pi$ pulse causes a $2\pi$ rotation and gives a $\pi$ phase shift to the original state. This conditional phase flip ($\pi$ rotation around the $z$ axis in the Bloch sphere) is converted into a conditional bit flip ($\pi$ rotation around a horizontal axis in the Bloch sphere) by the two $\pi/2$ pulses.

Figure 4(b) shows the result of the Cirac-Zoller gate experiment. Here the phase of the second pulse is rotated from 0 to $4\pi$ and the population in $|\uparrow\rangle$ is measured. Crosses represent the $|0\rangle$ preparation case, and filled circles the $|1\rangle$ preparation case. The interference fringes for the two cases clearly show a $\pi$ phase difference to each other, which is evidence of conditional dynamics caused by the BSB $2\pi$ pulse. The contrasts of the fringes are limited to 0.4–0.6, and for the BSB preparation case there is a negative offset of ~0.05, which is consistently observed in similar measurements. These imperfections are explained later.

### C. Numerical simulation

Numerical simulation is performed to quantitatively analyze the CZ gate result and to estimate possible fidelity for Bell state generation. A Liouville equation with exponential decay is solved for three internal levels ($|g\rangle$, $|\uparrow\rangle$, and $|\downarrow\rangle$) and five external levels representing the axial motional states truncated at $n_z = 4$. Coupling between the internal and external states is considered to the second order of the Lamb-Dicke factor $\eta$ for carrier excitation and to the first order for sideband excitation.

Fidelity-limiting factors except for that from axial motional state distribution, which include laser phase fluctuation and magnetic field fluctuation, are incorporated into the equation as exponential decay of off-diagonal density matrix elements for the internal degrees of freedom. For the axial motional state, the initial distribution is assumed to be a thermal distribution based on the experimental results of sideband cooling ($\overline{n_z} \sim 0.02$). Heating during the gate operation is neglected, which is reasonable since our measured heating rate is ~0.005 quanta/ms for the axial motion and the typical gate sequences are shorter than 1 ms.

The parameters for the exponential dephasing are extracted from experimental results by fitting simulation results for simple one-pulse sequences to the experimental Rabi oscillation results with the Rabi frequencies and the dephasing rates as fitting parameters. The dashed curves in Fig. 3 represent such fitted simulation results. By representing exponential decay of off-diagonal density matrix elements using a proportionality factor $\exp[-(\gamma/2)t]$, the values of $\gamma$ are extracted to be $2\pi \times 240$ Hz for $|g\rangle$–$|\uparrow\rangle$ and $2\pi \times 310$ Hz for $|\uparrow\rangle$–$|\downarrow\rangle$.

Based on the aforementioned assumptions, the CZ gate experiment is simulated with four pulses, and the result is shown in the Fig. 4(b) as curves. It reproduces well the reduction of fringe contrasts and also the negative offset in the case of $|1\rangle$ preparation without any fitting parameters except for a common phase offset ($\sim 2\pi \times 0.13$ rad). The negative offset is presumably caused by the infidelity in the BSB excitation on $|g\rangle$–$|\uparrow\rangle$ for the first and the third pulses. The infidelity results in population left in $|g\rangle$, which is considered as a leakage out of the computational subspace spanned by $|\uparrow\rangle$, $|\downarrow\rangle$ leading to a signal decrease.

The phase offset is considered to be caused by ac Stark shifts due to the applied optical pulses. In the case of quadrupole BSB excitation, the existence of the off-resonant carrier causes ac Stark shifts, which might be compensated for with an additional off-resonant beam [24]. In the case of stimulated Raman excitation, the two Raman beams off-resonant from

dipole transitions cause ac Stark shifts, which might be canceled by adjusting the power balance between the two beams [25]. In our estimation phase offset due to these shifts is below $2\pi \times 0.3$ rad and is considered to be responsible for the observed shift of $2\pi \times 0.13$ rad. This phase offset is common for both the $|0\rangle$ and $|1\rangle$ preparation cases and hence does not affect our interpretation of the conditional phase shift.

## IV. DISCUSSION

The conditional phase shift confirmed here is an essential result characterizing the CZ gate scheme, while the whole functionality of the gate operation may be examined thoroughly through performing quantum state or process tomography [26,27]. However, tomography on a single ion becomes relatively complicated since the motional qubit cannot be directly manipulated or measured and swapping it with the internal states is required to perform the desired operations [27]. Instead of performing tomography, here we numerically simulate Bell state generation using the CZ gate and estimate the fidelity to confirm the functionality of the gate.

A Bell state $|\Psi_B\rangle = (1/\sqrt{2})(|0\rangle|\uparrow\rangle + |1\rangle|\downarrow\rangle)$ can be produced from an initial state $|g\rangle$ by first applying a $\pi/2$ carrier pulse and a $\pi$ BSB pulse on $|g\rangle$–$|\uparrow\rangle$ to prepare $(1/\sqrt{2})(|0\rangle + |1\rangle)|\uparrow\rangle$ and then performing a controlled NOT operation that flips the internal qubit conditioned on the motional state. By using exactly the same parameters as used for the simulation in Fig. 4(b), the time dependence of the density matrix in the process of the generation of the Bell state $|\Psi_B\rangle$ is simulated. The fidelity of the final state $F \equiv \langle\Psi_B|\rho|\Psi_B\rangle$ is obtained as 0.77, which well exceeds the value 0.5 expected for product states [28].

Loss of fidelity in the Bell state generation process can be also estimated by simulation. Infidelity in excitation of the stimulated Raman transition $|\uparrow\rangle$–$|\downarrow\rangle$, which includes phase noise between the lasers and magnetic field fluctuation, contributes 15%–17%. Infidelity in excitation of $|g\rangle$–$|\uparrow\rangle$, which includes the 729-nm laser frequency noise and magnetic field fluctuation, contributes 4%–6%. Axial quantum number distribution contributes 2%. Intensity fluctuation is estimated to contribute as little as 0.1%, and the effect of spontaneous emission is ~0.1%.

## V. CONCLUSION

In conclusion, a quantum gate is demonstrated with an atomic qubit consisting of electronically excited states with a separation on the order of a terahertz. Conditional dynamics is clearly observed as a fringe reversal in Ramsey interferometry. Fidelity for Bell state generation is estimated to be 0.77, and decoherence factors are analyzed. The excitation scheme using stimulated Raman transitions with phase-locked lasers offers much flexibility and could eventually be used for atomic transitions that have not been explored before as qubit transitions as well as for molecular transitions.

## ACKNOWLEDGMENTS

We thank I. Chuang and his group for their cooperation in the development of the pulse programming system.

[1] R. Blatt and D. Wineland, Nature (London) **453**, 1008 (2008).
[2] H. Häffner, C. F. Roos, and R. Blatt, Phys. Rep. **469**, 155 (2008).
[3] S. A. Diddams, D. J. Jones, J. Ye, S. T. Cundiff, J. L. Hall, J. K. Ranka, R. S. Windeler, R. Holzwarth, T. Udem, and T. W. Hänsch, Phys. Rev. Lett. **84**, 5102 (2000).
[4] T. Udem, R. Holzwarth, and T. W. Hänsch, Nature (London) **416**, 233 (2002).
[5] M. Kourogi, K. Nakagawa, and M. Ohtsu, IEEE J. Quantum Electron. **29**, 2693 (1993).
[6] K. K. Ni, S. Ospelkaus, M. H. G. de Miranda, A. Pe'er, B. Neyenhuis, J. J. Zirbel, S. Kotochigova, P. S. Julienne, D. S. Jin, and J. Ye, Science **322**, 231 (2008).
[7] J. G. Danzl, E. Haller, M. Gustavsson, M. J. Mark, R. Hart, N. Bouloufa, O. Dulieu, H. Ritsch, and H. C. Nägerl, Science **321**, 1062 (2008).
[8] F. Lang, K. Winkler, C. Strauss, R. Grimm, and J. Hecker Denschlag, Phys. Rev. Lett. **101**, 133005 (2008).
[9] J. Deiglmayr, A. Grochola, M. Repp, K. Mörtlbauer, C. Glück, J. Lange, O. Dulieu, R. Wester, and M. Weidemüller, Phys. Rev. Lett. **101**, 133004 (2008).
[10] L. D. Carr, D. DeMille, R. V. Krems, and J. Ye, New J. Phys. **11**, 055049 (2009).
[11] C. Lee and E. A. Ostrovskaya, Phys. Rev. A **72**, 062321 (2005).
[12] S. F. Yelin, K. Kirby, and R. Cote, Phys. Rev. A **74**, 050301(R) (2006).
[13] E. Charron, P. Milman, A. Keller, and O. Atabek, Phys. Rev. A **75**, 033414 (2007).
[14] A. Kreuter, C. Becher, G. P. T. Lancaster, A. B. Mundt, C. Russo, H. Häffner, C. Roos, W. Hänsel, F. Schmidt-Kaler, R. Blatt, and M. S. Safronova, Phys. Rev. A **71**, 032504 (2005).
[15] J. I. Cirac and P. Zoller, Phys. Rev. Lett. **74**, 4091 (1995).
[16] C. Monroe, D. M. Meekhof, B. E. King, W. M. Itano, and D. J. Wineland, Phys. Rev. Lett. **75**, 4714 (1995).
[17] F. Schmidt-Kaler, H. Häffner, M. Riebe, S. Gulde, G. P. T. Lancaster, T. Deuschle, C. Becher, C. F. Roos, J. Eschner, and R. Blatt, Nature (London) **422**, 408 (2003).
[18] D. P. DiVincenzo, Phys. Rev. A **51**, 1015 (1995).
[19] A. Barenco, D. Deutsch, A. Ekert, and R. Jozsa, Phys. Rev. Lett. **74**, 4083 (1995).
[20] A. Barenco, C. H. Bennett, R. Cleve, D. P. DiVincenzo, N. Margolus, P. Shor, T. Sleator, J. A. Smolin, and H. Weinfurter, Phys. Rev. A **52**, 3457 (1995).
[21] R. Yamazaki, T. Iwai, K. Toyoda, and S. Urabe, Opt. Lett. **32**, 2085 (2007).
[22] J. L. Hall and T. W. Hänsch, Opt. Lett. **9**, 502 (1984).

[23] K. Toyoda, H. Shiibara, S. Haze, R. Yamazaki, and S. Urabe, Phys. Rev. A **79**, 023419 (2009).

[24] H. Häffner, S. Gulde, M. Riebe, G. Lancaster, C. Becher, J. Eschner, F. Schmidt-Kaler, and R. Blatt, Phys. Rev. Lett. **90**, 143602 (2003).

[25] S. Haze, R. Yamazaki, K. Toyoda, and S. Urabe, Phys. Rev. A **80**, 053408 (2009).

[26] M. Riebe, K. Kim, P. Schindler, T. Monz, P. O. Schmidt, T. K. Körber, W. Hänsel, H. Häffner, C. F. Roos, and R. Blatt, Phys. Rev. Lett. **97**, 220407 (2006).

[27] S. X. Wang, J. Labaziewicz, Y. Ge, R. Shewmon, and I. L. Chuang, e-print arXiv:0912.4892.

[28] C. A. Sackett *et al.*, Nature (London) **404**, 256 (2000).